

Examination of the Subsarcolemmal Tubular System of Mammalian Skeletal Muscle Fibers

Isuru D. Jayasinghe,[†] Harriet P. Lo,[‡] Garry P. Morgan,[§] David Baddeley,[¶] Robert G. Parton,[‡] Christian Soeller,^{¶**} and Bradley S. Launikonis^{†*}

[†]School of Biomedical Sciences, Faculty of Science, [‡]School of Molecular and Microbial Sciences, and [§]Institute for Molecular Bioscience and Centre for Microscopy and Microanalysis, The University of Queensland, Brisbane, Australia; [¶]School of Medical Sciences, Faculty of Medical and Health Sciences, University of Auckland, Auckland, New Zealand; ^{||}Department of Cell Biology, Yale University, New Haven; and ^{**}School of Physics, The University of Exeter, United Kingdom

ABSTRACT A subsarcolemmal tubular system network (SSTN) has been detected in skeletal muscle fibers by confocal imaging after the removal of the sarcolemma. Here we confirm the existence and resolve the fine architecture and the localization of the SSTN at an unprecedented level of detail by examining extracellularly applied tubular system markers in skeletal muscle fiber preparations with a combination of three imaging modalities: confocal fluorescence microscopy, direct stochastic optical reconstruction microscopy, and tomographic electron microscopy. Three-dimensional reconstructions showed that the SSTN was a dense two-dimensional network within the subsarcolemmal space around the fiber, running ~500–600 nm underneath and parallel to the sarcolemma. The SSTN is composed of tubules ~95 nm in width with ~60% of the tubules directed transversely and >30% directed longitudinally. The deeper regular transverse tubules located at each A-I boundary of the sarcomeres branched from the SSTN, indicating individual transverse tubules that form triads are continuous with, but do not directly contact the sarcolemma. This suggests that the SSTN plays an important role in affecting the exchange of deeper tubule lumina with the extracellular space.

Received for publication 30 November 2012 and in final form 16 April 2013.

*Correspondence: b.launikonis@uq.edu.au

The tubular (t-) system arises from regular invaginations of the surface membrane (sarcolemma) of skeletal muscle, forming a highly organized internal network of parallel membranous tubules that reach each sarcomere. The majority of the t-system comprises transversely arranged tubules which, in mammalian skeletal muscle, are located close to each of the A and I bands of the sarcomere (1). The direct continuity between its membranes and the surface sarcolemma allows the fast propagation of the action potentials deeper in to the interior of muscle fibers for supporting rapid excitation-contraction coupling (2). Less abundant longitudinal tubules of the t-system network can facilitate the axial propagation of excitation (1–4) but may also have other roles (5).

From confocal imaging of the t-system of mechanically skinned fibers, where the sarcolemma is removed, a network of tubules that connects the sarcolemma to t-system proper was identified, described as the subsarcolemmal tubular network (SSTN) (2,6). Little is known of the structure or indeed its functional role in muscle. Here we establish its presence in both skinned and intact muscle fibers and examine the architecture of the t-system immediately beneath the surface sarcolemma in detail, through three-dimensional fluorescence confocal imaging, direct stochastic optical reconstruction microscopy (dSTORM) super-resolution imaging, and tomographic electron microscopy (EM).

To visualize the t-system in skeletal muscle, adult rat extensor digitorum longus fibers were exposed to a Na⁺-based Ringer's solution (see the [Supporting Material](#)) containing 10 mM Fluo-5N salt. Fibers were then mechanically

skinned under liquid paraffin, transferred to a standard internal solution, and imaged using a confocal microscope (see the [Supporting Material](#)). Highly organized rows of transverse tubule doublets are seen throughout the interior regions (*right*) in a single longitudinal confocal section near the surface of a fiber ([Fig. 1 A](#)). Intensely fluorescent mesh-like morphology is observed at the curved surface of the skinned fiber that is in focus (highlighted with *box*). The strong infiltration of the membrane impermeable Fluo-5N into this network and its presence after mechanical skinning was highly suggestive that it was a membrane-bound compartment continuous with the t-system and with direct access to the outside of the fiber before mechanical skinning. A magnified view of a two-dimensional maximum intensity projection of the curved surface of the fiber within the indicated region in panel A revealed the SSTN comprised of an intricate two-dimensional network that appeared to wrap around the skinned fiber ([Fig. 1 B](#)). The two-dimensional projections of the SSTN were skeletonized and analyzed for directionality of the tubules (see the [Supporting Material](#) for image analysis). The histogram in [Fig. 1 C](#) illustrates the percentage of tubules detected in the skeletonization as a function of their angle relative to the transverse plane (0°). Two major peaks centering

Editor: Andrew McCulloch.

© 2013 by the Biophysical Society

<http://dx.doi.org/10.1016/j.bpj.2013.04.029>



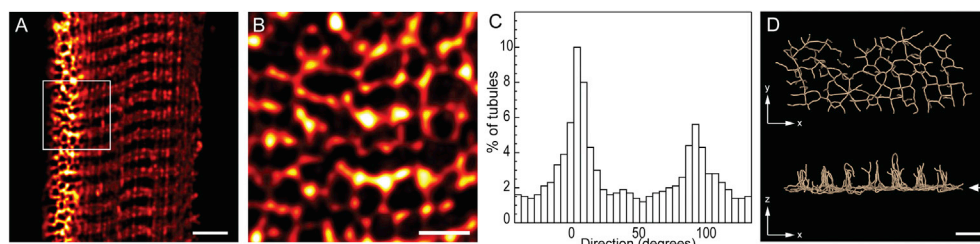


FIGURE 1 Diffraction-limited three-dimensional confocal imaging of the SSTN in rat fibers. (A) A single confocal section with a glancing view of the surface of a mechanically skinned fiber with Fluo-5N trapped within the sealed SSTN and t-system. A dense two-dimensional network was observed along the curved surface of the skinned fiber (*left margin*) that is in focus, in contrast to the tubular network deeper in the interior that follows a predominantly banded morphology (*right*). (B) A projection of the outermost 0.5 μm of the fiber within the region (shown by the *box* in panel A) indicates the complex SSTN. (C) A directionality analysis of a two-dimensional skeleton of the SSTN illustrates the percentage of tubules as a function of their orientation relative to the transverse plane. Only ~60% of the SSTN connections extended in the transverse direction ($\sim 0^\circ$). (D) *xy* (*upper*) and *xz* views (*lower*) of three-dimensional skeletonization of confocal image stacks emphasized the continuity of the SSTN with the t-tubules that are located periodically at the A-I junctions. (*Arrowhead*) Reference point to surface of the fiber. (Scale bars: A and D, 2 μm ; B, 1 μm .)

on 0° and 90° were observed, corresponding to tubules respectively aligned transversely and longitudinally. The integral of the peak centering on 0° was ~60% whereas the second peak corresponding to longitudinal tubules included >30% of all subsarcolemmal tubules. This shows a distinctly different organization of tubules in the transverse plane compared to the deeper transverse tubules. Three-dimensional skeletonization of confocal z-stacks illustrates the two-dimensional connectivity of this network along the surface of the skinned fiber (*xy* view in Fig. 1 D) and its continuity with underlying transverse tubules extending deeper into the fiber (*xz* view).

To further resolve the SSTN, the t-system of adult rat extensor digitorum longus fibers was infiltrated with 5 mM fixable dextran-linked Alexa680. After mechanical skinning, fibers were fixed in 4% (w/v) paraformaldehyde in phosphate-buffered saline. dSTORM was performed in an optical plane focused on the bottom surface of the skinned fiber. Fig. 2, A and B, illustrates the reconstructed grayscale dSTORM image of a region similar to that imaged by confocal microscopy in Fig. 1 B, with an improvement in resolution to ~30–40 nm. Similar to the confocal images, a complex two-dimensional network was observed in the space between the myofibrils and from where the sarcolemma had been removed. The highly continuous mesh-like appearance of resolved structures in these images is consistent with the morphology underlying the Fluo-5N fluorescence in the confocal images (Fig. 1) of SSTN

extending around the skinned fiber. A similar morphology was observed in cut fibers (with surface sarcolemma intact), with both confocal and dSTORM imaging techniques (see Fig. S1 in the Supporting Material).

A Euclidean distance analysis of the tubular connections stained with the dextran in dSTORM images was used for estimating the local tubule widths (see the Supporting Material). The histogram of the widths of subsarcolemmal tubules showed that they range between ~30 and 180 nm with a mean of ~94 nm (Fig. 2 C).

Tomographic EM of mouse flexor digitorum brevis fibers was used for visualizing the fine geometry of the SSTN. The t-tubules of enzymatically isolated fibers were infiltrated with Ruthenium red before fixation and sectioning (see the Supporting Material). A series of planes from a tomogram (Fig. 3 A) shows the continuity between deeper transverse tubules and subsarcolemmal tubule located ~600 nm underneath and parallel to the fiber's surface (*i–iii*). Panel *iv* and the maximum intensity projection in Fig. 3 B illustrate the short tubules that connect the SSTN to the surface sarcolemma.

The small cytoplasmic gap between the SSTN and the surface sarcolemma could explain why this network was not previously detected with diffraction-limited light microscopies that lack the axial resolution or standard thin-section EM. The ultrastructure of SSTN described here with three imaging modalities is consistent with convolutions, dilatations, or kinks of the transverse tubules

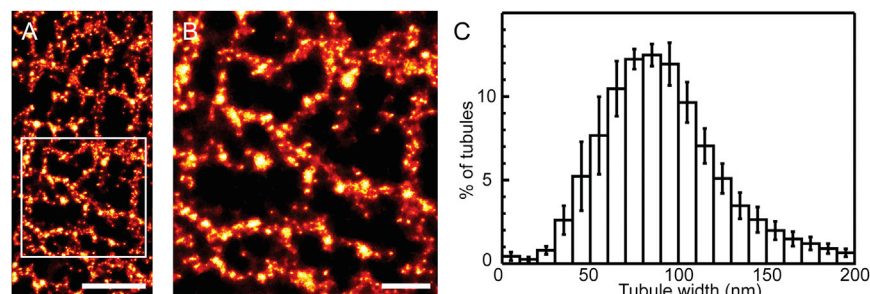


FIGURE 2 dSTORM imaging of the SSTN in rat fibers. (A) dSTORM reconstruction of dextran-linked Alexa680 trapped within the sealed SSTN in a mechanically skinned fiber. (B) A magnified view of the subsarcolemmal tubules. (C) The distribution of SSTN tubule widths. Mean width: 94.28 ± 8.54 nm; mean \pm SE; $n = 6$ fibers, 3 animals. (Scale bars: A, 1 μm and B, 500 nm.)

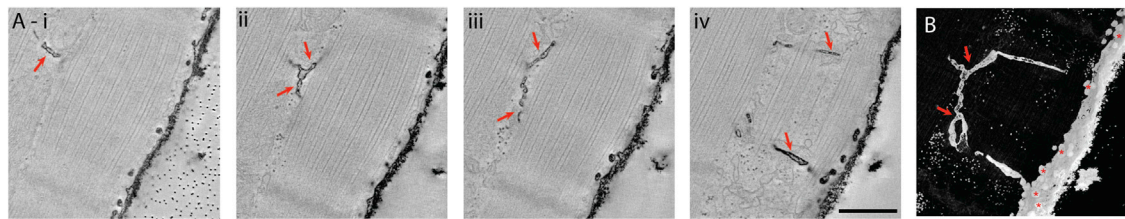


FIGURE 3 Tomographic EM analysis of subsarcolemmal tubules. (A) A series of planes spaced at 75 nm within an EM tomogram of a 300-nm-thick section of a mouse flexor digitorum brevis fiber where sarcolemmal and tubular membranes were stained with Ruthenium red. (Arrows) Continuity of transverse tubules to a longitudinal tubule of the SSTN (*i* and *ii*), which connects to the surface sarcolemma via short (~600 nm) tubular connections (*iii* and *iv*). (Scale bar: 500 nm.) (B) A maximum intensity projection of the intensity-inverted tomogram illustrates the localizations of the subsarcolemmal tubules (arrows), which are distinct from the caveolae observed at the surface sarcolemma (asterisks).

observed near the fiber surface in 500 Å sections of rat (7) and frog muscle (8). In size, the widths of the tubules estimated using dSTORM (Fig. 2 C) are larger (~50–100%) than previous estimates using EM (9). This discrepancy could indicate the presence of wider tubules within the SSTN compared to the t-system or a flattened cross-sectional shape that would overrepresent their diameters in longitudinal two-dimensional dSTORM images.

The functional role of the SSTN is not clear. A direct role in Ca^{2+} release seems unlikely. It is possible that these tubules are the remnants of the earliest elements of the tubular network during development that consists largely of longitudinal tubules near the surface sarcolemma (6,10). Its continuity with the extracellular space and deeper t-system could allow it to serve as a membrane reservoir for ongoing remodeling of the deeper t-system, perhaps in conjunction with fiber hypertrophy. The tortuosity that the SSTN adds to the t-system is likely to affect diffusion between the extracellular space and deeper t-tubules. For example, this may allow the SSTN to buffer any accumulating K^{+} or metabolites during high-frequency contractions. Its structure as a mesh surrounding the myofibrillar space also gives it a potential role in ensuring fiber excitability (2) or mechanosensation. Examining the spatial distributions of ion channels, transporters, and signaling molecules in SSTN membranes should help further understanding of the functional role of these tubules.

Our data confirm previous observations (2,6) of the SSTN and we provide the first quantitative description, to our knowledge, of its structure. Importantly, preservation of the SSTN in skinned fibers will facilitate investigation into its function.

SUPPORTING MATERIAL

Materials, methods, two figures, and references (10–13) are available at [http://www.biophysj.org/biophysj/supplemental/S0006-3495\(13\)00462-1](http://www.biophysj.org/biophysj/supplemental/S0006-3495(13)00462-1).

ACKNOWLEDGMENTS

Authors acknowledge the financial support by the Australian Research Council and the use of the Australian Microscopy & Microanalysis Research Facility at the Center for Microscopy and Microanalysis,

University of Queensland. This work was also supported by Muscular Dystrophy Queensland and Brain Foundation grants to B.S.L. The Institute for Molecular Bioscience is a Special Research Center of the Australian Research Council.

REFERENCES and FOOTNOTES

1. Franzini-Armstrong, C., D. G. Ferguson, and C. Champ. 1988. Discrimination between fast- and slow-twitch fibers of guinea pig skeletal muscle using the relative surface density of junctional transverse tubule membrane. *J. Muscle Res. Cell Motil.* 9:403–414.
2. Edwards, J. N., T. R. Cully, ..., B. S. Launikonis. 2012. Longitudinal and transversal propagation of excitation along the tubular system of rat fast-twitch muscle fibers studied by high speed confocal microscopy. *J. Physiol.* 590:475–492.
3. Posterino, G. S., G. D. Lamb, and D. G. Stephenson. 2000. Twitch and tetanic force responses and longitudinal propagation of action potentials in skinned skeletal muscle fibers of the rat. *J. Physiol.* 527:131–137.
4. Veratti, E. 1961. Investigations on the fine structure of striated muscle fiber read before the Reale Istituto Lombardo, 13 March 1902. *J. Biophys. Biochem. Cytol.* 10(4, Suppl):1–59.
5. Edwards, J. N., and B. S. Launikonis. 2008. The accessibility and interconnectivity of the tubular system network in toad skeletal muscle. *J. Physiol.* 586:5077–5089.
6. Murphy, R. M., J. P. Mollica, and G. D. Lamb. 2009. Plasma membrane removal in rat skeletal muscle fibers reveals caveolin-3 hot-spots at the necks of transverse tubules. *Exp. Cell Res.* 315:1015–1028.
7. Walker, S. M., and G. R. Schrodt. 1965. Continuity of the t-system with the sarcolemma in rat skeletal muscle fibers. *J. Cell Biol.* 27:671–677.
8. Franzini-Armstrong, C., L. Landmesser, and G. Pilar. 1975. Size and shape of transverse tubule openings in frog twitch muscle fibers. *J. Cell Biol.* 64:493–497.
9. Dulhunty, A. F. 1984. Heterogeneity of t-tubule geometry in vertebrate skeletal muscle fibers. *J. Muscle Res. Cell Motil.* 5:333–347.
10. Takekura, H., B. E. Flucher, and C. Franzini-Armstrong. 2001. Sequential docking, molecular differentiation, and positioning of t-tubule/SR junctions in developing mouse skeletal muscle. *Dev. Biol.* 239:204–214.
11. Wagner, E., M. A. Lauterbach, ..., S. E. Lehnart. 2012. Stimulated emission depletion live-cell super-resolution imaging shows proliferative remodeling of t-tubule membrane structures after myocardial infarction. *Circ. Res.* 111:402–414.
12. Baddeley, D., I. D. Jayasinghe, ..., C. Soeller. 2009. Optical single-channel resolution imaging of the ryanodine receptor distribution in rat cardiac myocytes. *Proc. Natl. Acad. Sci. USA* 106:22275–22280.
13. Meng, E. C., E. F. Pettersen, ..., T. E. Ferrin. 2006. Tools for integrated sequence-structure analysis with UCSF Chimera. *BMC Bioinformatics.* 7:339.